

12-2001

# Dark Production: A Significant Source of Oceanic COS


M. Von Hobe

Gregory A. Cutter  
*Old Dominion University*, [gcutter@odu.edu](mailto:gcutter@odu.edu)

A. J. Kettle

M. O. Andreae

Follow this and additional works at: [https://digitalcommons.odu.edu/oeas\\_fac\\_pubs](https://digitalcommons.odu.edu/oeas_fac_pubs)

 Part of the [Atmospheric Sciences Commons](#), [Biogeochemistry Commons](#), and the [Oceanography Commons](#)

---

## Repository Citation

Von Hobe, M.; Cutter, Gregory A.; Kettle, A. J.; and Andreae, M. O., "Dark Production: A Significant Source of Oceanic COS" (2001). *OEAS Faculty Publications*. 49.  
[https://digitalcommons.odu.edu/oeas\\_fac\\_pubs/49](https://digitalcommons.odu.edu/oeas_fac_pubs/49)

## Original Publication Citation

Von Hobe, M., Cutter, G., Kettle, A., & Andreae, M. (2001). Dark production: A significant source of oceanic cos. *Journal of Geophysical Research: Oceans*, 106(C12), 31217-31226. doi: 10.1029/2000JC000567

## Dark production: A significant source of oceanic COS

M. Von Hobe<sup>1</sup>

Biogeochemistry Department, Max Planck Institute for Chemistry, Mainz, Germany

G. A. Cutter

Department of Ocean, Earth, and Atmospheric Sciences, Old Dominion University, Norfolk, Virginia, USA

A. J. Kettle and M. O. Andreae

Biogeochemistry Department, Max Planck Institute for Chemistry, Mainz, Germany

**Abstract.** Carbonyl sulfide (COS) in air and dissolved in seawater was determined during a cruise in August 1999 in the Sargasso Sea in the northwest Atlantic Ocean. Dissolved concentrations at the sea surface displayed only a weak diel cycle with a mean of  $8.6 \pm 2.8$  pmol  $\text{dm}^{-3}$  owing to low abundance of photochemical precursors and high temperatures causing rapid hydrolysis. Depth profiles measured over the oceanic mixed layer revealed significant vertical gradients of COS concentration with higher values at the surface, suggesting that the rate of photochemical production at the surface exceeds the rate of vertical mixing. The mean atmospheric mixing ratio was  $486 \pm 40$  ppt, and calculated sea-air fluxes ranged from 0.03 to 0.8 g COS  $\text{km}^{-2} \text{d}^{-1}$ . COS dark production, estimated from the predawn COS concentration at the surface and the hydrolysis constant, contributed significantly to the total amount of COS produced. A strong temperature dependence of the COS dark production rate  $q$  was found by comparing previously published values. The data further indicate an approximately first-order relationship between  $q$  and chromophoric dissolved organic matter (CDOM) absorbance at 350 nm,  $a_{350}$ , which is used as a proxy for the CDOM content of the water but is likely to covary with other parameters, such as biological activity, that could also affect COS dark production. Together with known functions for COS hydrolysis and solubility, the parameterization of dark production as a function of temperature and  $a_{350}$  allows for the prediction of COS concentrations and saturation ratios as a function of physical and optical seawater properties in the absence of photoproduction. This is used to estimate a lower limit of 0.056 Tg COS  $\text{yr}^{-1}$  to the annual COS flux from the ocean to the atmosphere.

### 1. Introduction

Carbonyl sulfide (COS) is the most abundant reduced sulfur gas in the atmosphere. Its atmospheric burden is an estimated 5.2 Tg [Chin and Davis, 1995], and its average global mixing ratio ( $\sim 510$  ppt) shows relatively little spatial and temporal variability [Bandy *et al.*, 1992]. COS is chemically stable, and its atmospheric residence time is estimated to be  $\sim 6$  years [Ulshöfer and Andreae, 1998]. Therefore COS can be transported into the stratosphere, where it is photodissociated and oxidized to sulfur dioxide ( $\text{SO}_2$ ) and thus contributes to the stratospheric sulfate aerosol layer (also known as the Junge layer) in times of volcanic quiescence [Crutzen, 1976]. The importance of this layer for the Earth's climate by scattering incoming solar radiation [Turco *et al.*, 1980] and for heterogeneous ozone chemistry [Solomon *et al.*, 1993] has drawn much attention to the sources and sinks of COS.

Recent global COS budgets [Andreae and Crutzen, 1997; Watts, 2000] are balanced within the uncertainties of the individual source and sink terms. Watts [2000] estimates the annual flux from the open ocean to be  $0.10 \pm 0.15$  Tg COS  $\text{yr}^{-1}$ , which is

$<10\%$  of the total COS sources, but this flux is the source with the largest uncertainty. It is mainly the great spatial and temporal variability of COS in surface waters and, in the light of this variability, the small number of measurements that make it difficult to quantify the global oceanic flux. The variability in COS concentration results from the various competing removal and production processes that are sensitive to a great number of parameters. The main removal process, hydrolysis, strongly depends on temperature and, to a lesser extent, on salinity and pH [Elliott *et al.*, 1989; Radford-Knoery and Cutter, 1994]. Downward mixing and gas exchange, which can also remove COS from surface water, are greatly influenced by wind speed. The principal source of COS in the ocean is photochemical production from chromophoric dissolved organic matter (CDOM) [Ferek and Andreae, 1984]. The magnitude of this source depends on solar irradiance, seawater absorption, and CDOM content [Ulshöfer and Andreae, 1998]. Because photochemical production is limited to the photic zone, COS concentrations at the surface are usually higher than below.

One source of COS that has been recognized [Flöck and Andreae, 1996; Radford-Knoery and Cutter, 1994; Ulshöfer *et al.*, 1996] but has received little attention is production in the absence of light, so-called dark production. On the basis of the microbial production of COS in marine sediments [Zhang *et al.*, 1998], Radford-Knoery and Cutter [1994] suggested that COS production well below the euphotic zone could be coupled with organic matter regeneration. Flöck *et al.* [1997] proposed a radical pathway similar to the photoproduction process [Flöck

<sup>1</sup>Now at Forschungszentrum Jülich, ICG-I, Jülich, Germany.

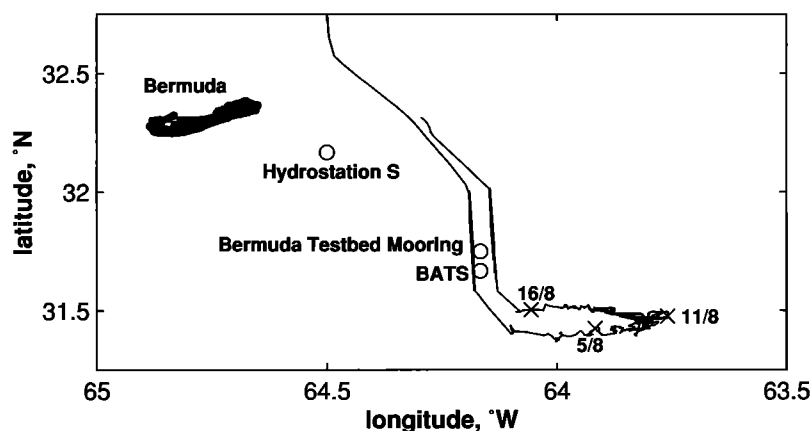


Figure 1. Cruise track with position at 1200 UT on selected days (solid crosses).

*et al.*, 1997; *Pos et al.*, 1998], for example, with thiyl radicals formed in the dark by either electron transfer from thiolate anions to oxygen [Ohno, 1977] or metal catalyzed auto-oxidation [Leung and Hoffmann, 1988]. However, neither of these potential production mechanisms has been quantitatively evaluated in the open ocean.

This paper examines the dynamics of COS cycling in the Sargasso Sea during the summer when elevated temperatures and a long period of daylight in the shallow mixed layer provide a distinct contrast to underlying thermocline waters where the only inputs of COS should be mixing and dark production. Using the results from this campaign and previous studies reporting COS dark production, an attempt is made to parameterize the dark production rate in terms of easily measurable variables and to assess its significance on a local and global scale.

## 2. Experiment

### 2.1. Study Period and Area

Measurements were taken from August 7 to 16, 1999, on board the R/V *Endeavor*, keeping a drift station at approximately 31°N, 63.5°W, which is just southeast of the Bermuda Atlantic Time Series Station (BATS) (Figure 1). The ship followed a subsurface drogue to stay with the same water mass.

### 2.2. Seawater Characteristics and Meteorological Conditions

Seawater pH was determined spectrophotometrically according to a method by Clayton and Byrne [1993]. Seawater absorbance spectra were measured by N. Nelson from the Bermuda Biological Station for Research (St. George's, Bermuda). Other properties of the water mass, including conductivity-temperature-depth (CTD) profiles, and meteorological data were provided by the ship's systems and are summarized in Table 1. All data are in good agreement with long-term climatological averages reported for the BATS region in August (Table 1).

### 2.3. COS Determination

Atmospheric and dissolved COS concentrations were determined using an automated analytical system with cryogenic preconcentration, gas chromatographic separation, and flame photometric detection (cryotrap-GC/FPD). This system was originally designed by Ulshöfer *et al.* [1995] but was modified by Von Hobe *et al.* [2000]. Ambient air was sampled at 5 m above sea level and pumped to the analytical system through ~60 m

of PTFE tubing (outer diameter (OD) of 12.8 mm; inner diameter (ID) of 9.6 mm). Dissolved COS was determined by pumping the seawater through a Weiss-type equilibrator [Butler *et al.*, 1988; Weiss *et al.*, 1992] at 20 dm<sup>3</sup> min<sup>-1</sup> and analyzing the headspace. Seawater from the surface and depths down to 40 m, monitored by an SBE 19 CTD (Sea-Bird Electronics) connected to the sampling tube, was pumped to the equilibrator from a submersible pump (Grundfos, Wahlstedt, Germany) connected with 70 m of Guttasyn PVC tubing (OD of 34 mm; ID of 25 mm). There were times when the pump could not be deployed. Instead, water from the ship's seawater supply was used, resulting in a significant loss of COS due to hydrolysis for which the data had to be corrected (see Figure 2a). The correction function  $[\text{COS}]_{\text{aq}} = 1.62 [\text{COS}]_{\text{SSW}} - 1.93$  was determined from a least squares fit of  $[\text{COS}]_{\text{aq}}$  measured from samples drawn by the submersed pump versus  $[\text{COS}]_{\text{SSW}}$  at the times when the supply was switched. The general form of this relationship is typical for hydrolytic decay of COS in the ship's supply line. The subtractive term is rationalized by the fact that  $[\text{COS}]_{\text{aq}}$  and  $[\text{COS}]_{\text{SSW}}$  do not match each other at zero but at the equilibrium concentration reached between dark production and hydrolysis (see section 3.2). The numbers in the correction function suggest a delay of 2.7 hours in the ship's seawater pipes, which is longer than it should theoretically be, and an equilibrium concentration of 3.1 pmol dm<sup>-3</sup>, which is lower than the value determined below. Possible explanations include an enhanced hydrolysis rate due to some contamination in the ship's seawater supply and loss of COS by gas exchange with some low concentration headspace (the kinetics for such a process are analogous to those of the hydrolytic decay, with a subtractive term arising from a nonzero headspace concentration; see section 3.1).

After passing the air samples (0.3 dm<sup>3</sup> at STP, measured using a Tylan FC280S mass flow controller) through a Nafion drier, the sulfur compounds were trapped in a silanized glass-lined stainless steel tube (length of 20 cm; ID of 2 mm) filled with Chromosorb W (mesh 45/60, acid washed, DMCS treated) and cooled to -140°C by a CRYOTIGER electrical refrigerator (APD cryogenics, Allentown, Pennsylvania). The sample was injected onto the chromatographic column (length of 1.8 m; ID of 1.65 mm; PTFE; 60/80 Carboxpack II/1.5% XE 60/1.0% H<sub>3</sub>PO<sub>4</sub>) by electrically heating the trap. COS was separated from other sulfur compounds by a three-stage temperature program (1.8 min at 50°C, 30°C min<sup>-1</sup>; 2 min at 85°C, 30°C min<sup>-1</sup>; 2.5 min at 120°C) and detected flame photometrically. For the carrier gas, helium with <1 ppm total impurities and further cleaned in an activated charcoal/molecular sieve (5Å) scrubber was used; no carrier gas blank was detected. Standards

**Table 1.** Mean Values and Standard Deviations of COS Concentrations, Water Mass Characteristics, and Meteorological Data Measured During EN-327<sup>a</sup>

	EN-327	Climatological Average for August
COS measurements		
[COS] <sub>aq</sub> , pmol dm <sup>-3</sup>	8.6 ± 2.8 (n = 509)	...
[COS] <sub>atm</sub> , ppt	486 ± 40 (n = 167)	...
COS supersaturation (SR)	1.33 ± 0.38	...
F, g km <sup>-2</sup> d <sup>-1</sup>	0.24 ± 0.44	...
Seawater characteristics		
t <sub>seasurface</sub> , °C	27.4 ± 0.2	27.7 ± 0.8 <sup>b</sup>
salinity S	36.61 ± 0.06	36.45 ± 0.20 <sup>b</sup>
pH <sup>c</sup>	8.094 ± 0.015	
CDOM absorbance a <sub>CDOM</sub> at 350 nm, m <sup>-1</sup>	0.03	
Mixed layer depth d <sub>mix</sub> , m	15 ± 9	17 ± 9 <sup>b</sup>
Meteorological data		
Wind speed at 10 m u <sub>10</sub> , m s <sup>-1</sup>	4.5 ± 2.5	4.7 <sup>c</sup>
Wind direction	mainly NE-NW	mainly N <sup>d</sup>
Surface irradiance I, W m <sup>-2</sup>	246 ± 320	250 <sup>e</sup>
t <sub>air</sub> , °C	28.1 ± 0.9	27.2 <sup>d</sup>
Relative humidity, %	87 ± 4	80 <sup>d</sup>

<sup>a</sup> COS fluxes are calculated according to the model of *Nightingale et al.* [2000] (see section 3.4). Climatological averages for seawater properties and meteorological data of the region are given for comparison.

<sup>b</sup> Calculated averages for data extracted from the Bermuda Biological Station for Research website at <http://www.bbrs.edu/users/ctd>.

<sup>c</sup> On the total H scale [*Millero*, 1995].

<sup>d</sup> From Comprehensive Ocean-Atmosphere Data Set (COADS1) data provided by the National Oceanic and Atmospheric Administration (NOAA) Cooperative Institute for Research in Environmental Sciences (CIRES) Climate Diagnostics Center, Boulder, Colorado, from their Web site at <http://www.cdc.noaa.gov/>.

<sup>e</sup> From a global climatology of surface marine meteorological observations prepared by the by the National Climate Data Center (NCDC).

were prepared using gravimetrically calibrated COS permeation devices (permeation rates were 35.9 ± 0.2 and 10.9 ± 0.2 ng min<sup>-1</sup>) kept in a 25°C thermostated chamber constantly flushed with synthetic air. The detection limit (3σ) was ~30 pg COS, which corresponds to 30 ppt in air and 0.4 pmol dm<sup>-3</sup> in water for our sampling conditions. Reproducibility was better than 2%.

The system was capable of taking one measurement every 15 min. A 1 hour sampling routine of one air measurement followed by three seawater measurements was repeated continuously, except when depth profiles were measured.

### 3. Results and Discussion

#### 3.1. COS Concentrations and Sea-Air Flux

Figure 2a clearly shows the characteristic diel cycle in the surface concentration of dissolved COS. This cycle follows the surface solar irradiance with a time lag of ~2 hours. The amplitude of the diel variations is small with concentrations ranging from 4.4 to 17.9 pmol dm<sup>-3</sup>, the average concentration being 8.6 ± 2.8 pmol dm<sup>-3</sup>. This behavior is explained by the moderate COS photoproduction rates typically found in oligotrophic open ocean water with low abundance of photochemical precursors [*Ulshöfer*, 1995; *Von Hobe et al.*, 1999]. The fast hydrolysis rates at high temperatures also act to keep COS concentrations small.

Most depth profiles (Figure 3) show a higher COS concentration at the surface than at the bottom of or below the oceanic mixed layer (depth d<sub>mix</sub> shown in Table 2). The observed concentration gradients indicate that during most days, photoproduction is proceeding at a faster rate than downward mixing. This is not the case in the morning when the COS photo-produced during the previous day has been hydrolyzed or mixed and the concentration is nearly homogeneous (profile 4). Rapid breakdown of stratification was observed on August 9, 1999

(profiles 2 and 3) when wind speed was comparatively high (Table 2).

The mean atmospheric COS mixing ratio for the cruise was 486 ± 40 ppt, close to the average tropospheric mixing ratio of 510 ppt [*Bandy et al.*, 1992] and showing little variability (Figure 2b). There is no explanation for the large deviations observed on August 10, 13, and 14, but the rapid changes could indicate an error, such as contamination from the ship's exhaust or sea spray in the sampling line.

From surface seawater concentrations and atmospheric COS mixing ratios the gas exchange between the ocean and the atmosphere can be calculated using the stagnant film model, analogous to Fick's diffusion law [*Broecker and Peng*, 1974; *Liss and Slater*, 1974]. The sea-air flux *F* is given by

$$F = k_w(SR - 1) = k_w \left( [\text{COS}]_{\text{aq}} - \frac{[\text{COS}]_{\text{air}}}{H} \right), \quad (1)$$

where SR is the COS saturation ratio, [COS]<sub>aq</sub> and [COS]<sub>air</sub> are the COS concentrations in seawater and in air, *H* is the Henry's law constant, and *k<sub>w</sub>* is the exchange coefficient.

*H* was calculated as a function of seawater temperature and salinity according to *Ulshöfer et al.* [1995]. The exchange coefficient *k<sub>w</sub>* can be estimated as a function of wind speed at 10 m height by various empirical models, of which we used a relatively new one by *Nightingale et al.* [2000], which predicts a wind speed dependence intermediate between earlier published gas-exchange models [*Erickson*, 1993; *Liss and Merlivat*, 1986; *Wanninkhof*, 1992]. For the conditions during the expedition, this model gives *k<sub>w</sub>* values between 0 and 7.3 × 10<sup>-5</sup> m s<sup>-1</sup> with a mean of 1.7 × 10<sup>-5</sup> m s<sup>-1</sup>.

Figure 2c shows that during daytime, there was always a positive flux of COS from the ocean into the atmosphere. At night the ocean was slightly undersaturated in COS with respect to the atmosphere because of the fast hydrolysis rates, and a small flux

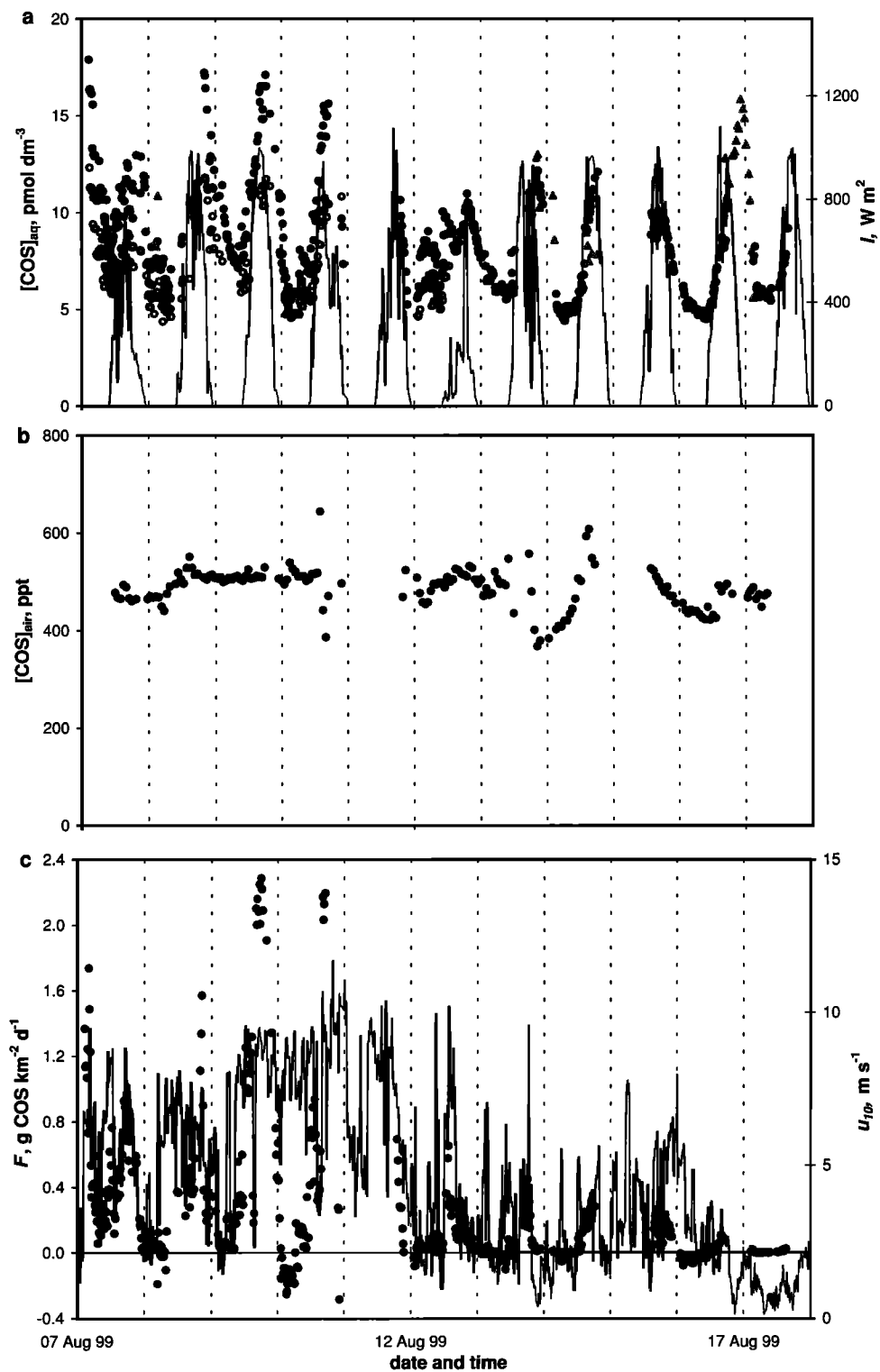


**Figure 2.** Time series for COS data and relevant parameters. Vertical gridlines indicate 0000 UT (5 hours ahead of local time). (a)  $[\text{COS}]_{\text{aq}}$  (solid circles) and surface solar irradiance (line). Open circles show uncorrected measurements of water pumped through the ship's seawater supply (SSW). The data were verified and supplemented with data measured by an independent sampling and analytical system shown as shaded triangles. This instrument measures with a reproducibility of better than 5% and is described in detail by Zhang *et al.* [1998] and Radford-Knoery and Cutter [1993]. (b)  $[\text{COS}]_{\text{air}}$ . (c) COS flux calculated from the Nightingale *et al.* [2000] gas exchange model (dots) and wind speed at 10 m height (line).

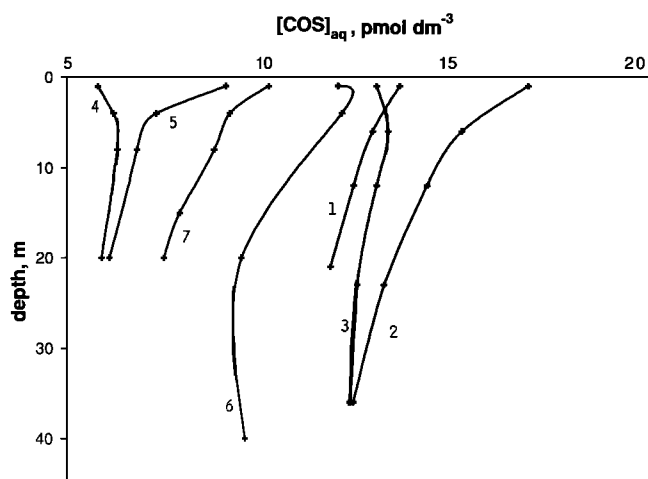


**Figure 3.**  $[\text{COS}]_{\text{aq}}$  depth profiles. Numbers in Figure 3 correspond to those given in Table 2.

from the atmosphere into the ocean was observed. During the second half of the cruise, wind speeds remained below  $5 \text{ m s}^{-1}$ , and as a consequence, fluxes were small. Daily COS fluxes into the atmosphere were determined by the integration of flux values over 24 hour periods and ranged from 0.03 to  $0.8 \text{ g COS km}^{-2} \text{ d}^{-1}$ , which is in the range of the average daily flux density ( $0.5 \text{ g COS km}^{-2} \text{ d}^{-1}$ ) reported for subtropical open ocean regions in summer [Ulshöfer and Andreae, 1998].

### 3.2. Role of COS Dark Production

While the maximum COS concentrations found at the surface and the amplitude of the observed diel cycle are rather moderate, the minimum COS concentrations measured before dawn remain relatively high in spite of the rapid hydrolysis. The hydrolysis rate constant  $k_h$  calculated as a function of the cruise average temperature, salinity, and pH is  $5.9 \times 10^{-5} \text{ s}^{-1}$  according to a formulation from Elliott *et al.* [1989] and  $4.6 \times 10^{-5} \text{ s}^{-1}$  according to Radford-Knoery and Cutter [1994], corresponding to COS lifetimes of 4.7 and 6.1 hours, respectively. With lifetimes as short as this the minimum COS concentration found early in the morning should approximately represent an equilibrium between hydrolysis and nonphotochemical production. Influx from the atmosphere can largely be ignored under the observed conditions: using  $4.4 \text{ pmol dm}^{-3}$  for predawn  $[\text{COS}]_{\text{aq}}$  and the average values given in Table 1 for  $[\text{COS}]_{\text{atm}}$ ,  $u_{10}$ ,  $t$ , and  $S$ , the increase in  $[\text{COS}]_{\text{aq}}$  for a 3 m thick layer (sampling depth) is  $0.01 \text{ pmol m}^{-3} \text{ s}^{-1}$ . The hydrolysis rate and therefore the rate of COS dark production is  $0.26 \text{ pmol m}^{-3}$

$\text{s}^{-1}$  using the Elliot formulation and  $0.20 \text{ pmol m}^{-3} \text{ s}^{-1}$  using the Radford-Knoery and Cutter formulation. This corresponds to a total daily dark production of  $22.4 \text{ pmol dm}^{-3} \text{ d}^{-1}$  and  $17.3 \text{ pmol dm}^{-3} \text{ d}^{-1}$ , respectively. To verify this rate for dark OCS production, incubations of unfiltered seawater were conducted in the dark to directly measure OCS production (G. A. Cutter, unpublished data, 1999). In this manner, dark OCS production was found to be  $36.7 \pm 11.5 \text{ pmol dm}^{-3} \text{ d}^{-1}$  ( $n = 12$ ), in reasonable agreement with the calculated values.

Depending on the amount of light available for photoproduction on each day, dark production makes up between 39 and 57% of the total amount of COS produced in the upper 5 m of the water column over the course of 1 day. Total production is assumed to be equivalent to the total amount of COS removed, calculated by integrating the rates of hydrolysis, sea-air gas exchange (see section 3.1), and downward mixing (approximated by eddy diffusion as described by Najjar *et al.* [1995]) over 1 day periods (only days with a complete COS time series are considered). Because the dark production rates are based on hydrolysis rates as described above and hydrolysis amounts to 90% or more of the total COS removal, the proportion of the total daily COS production that can be attributed to dark production according to the above calculation is largely independent of which hydrolysis formulation is used.

The strong contribution of dark to total COS production is probably related to the high seawater temperatures prevailing in the Sargasso Sea in summer and may be observed in other ocean areas with warm waters as well. It has been suggested that COS dark production varies with temperature by Ulshöfer [1995], who showed an Arrhenius dependence for his values obtained in the northeast Atlantic. Indeed, a temperature dependence of COS dark production would be expected for both mechanistic theories that have been proposed. If dark production was a microbial process [Radford-Knoery and Cutter, 1994; Zhang *et al.*, 1998], then increasing temperature would increase respiration and thus OCS production. In the proposed mechanism of COS dark production from dissolved organic matter (DOM) [Flöck *et al.*, 1997; Pos *et al.*, 1998], any nonphotochemical radical formation step requires thermal energy, leading to a temperature dependence.

In Figure 4, we show an Arrhenius dependence for reported values of the dark production rate (Table 3), scaled to the CDOM absorption at 350 nm, which has previously been hypothesized to correlate with COS dark production [Von Hobe *et al.*, 1999]. The Arrhenius fit yields the equation

$$\ln(q/a_{350}) = 51.1 - 14800 T^{-1}, \quad (2)$$

with a correlation coefficient  $r^2 = 0.75$  and a standard error of the estimate for  $q$  of 73%, where  $q$  is the dark production rate ( $\text{pmol m}^{-3} \text{ s}^{-1}$ ) and  $T$  is absolute temperature (K). If the three values, which are significantly outside the 95% confidence interval and have an error >100% (the uncertainty in the dark production rate is higher than the rate itself) are removed from

**Table 2.** Conditions at the Depth Profiling Stations

	Profile						
	1	2	3	4	5	6	7
Date	Aug. 7	Aug. 9	Aug. 9	Aug. 14	Aug. 14	Aug. 14	Aug. 17
Time, LT	1730	1600	1800	0800	0930	1430	1200
Latitude, °N	31.40	31.42	31.41	31.51	31.50	31.51	31.50
Longitude, °W	63.50	63.41	63.43	63.48	63.49	63.51	64.08
$I^a$ , $\text{MJ m}^{-2}$	12.8	24.2	26.1	1.3	4.3	20.2	11.1
$u_{10}$ , $\text{m s}^{-1}$	2.7	8.4	8.2	3.7	2.9	3.6	0.7
$d_{\text{mix}}$ , m	32	8	35	27	8	8	3

<sup>a</sup> Integrated from sunrise until the time when the depth profile was taken.

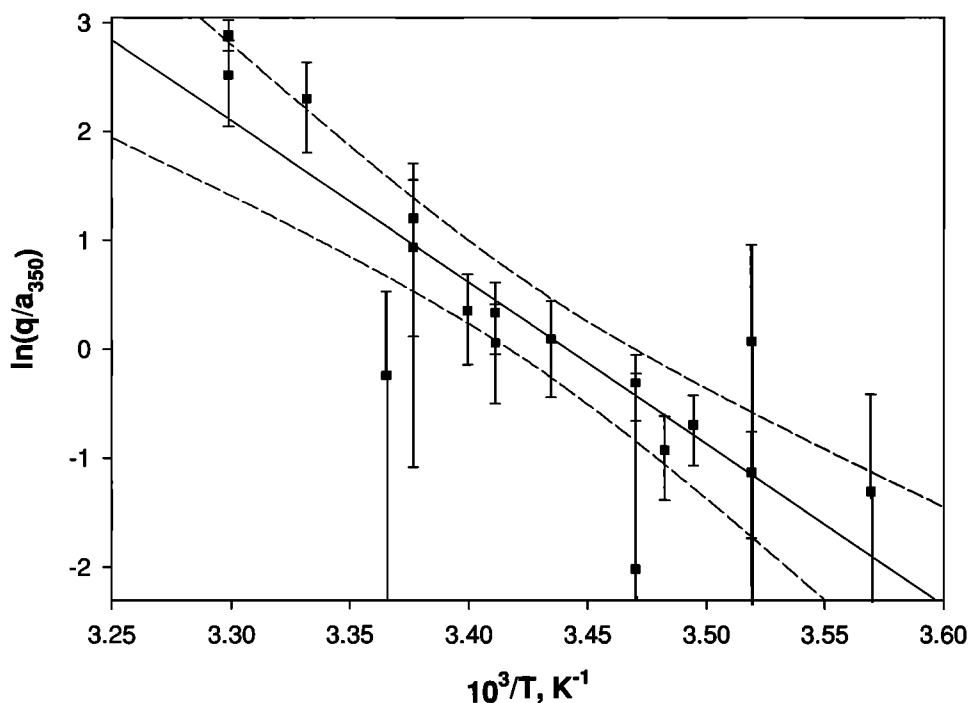


**Figure 4.** Arrhenius plot showing the temperature dependence of all reported COS dark production values scaled to  $a_{350}$ . Error bars account for errors in dark production rate determinations and  $a_{350}$  values. Where there was no error information, a 30% error was assumed on the basis of the approximate mean error from the other data. Only the values based on Elliot's hydrolysis parameterization is plotted for EN-327 because all the other referenced values are also based on this hydrolysis rate constant.

**Table 3.** EN-327 and Previously Published Values for COS Dark Production Rates<sup>a</sup>

Reference	Location <sup>b</sup>	Date	$q$ , $\text{pmol m}^{-3} \text{s}^{-1}$	SST, $^{\circ}\text{C}$	$a_{350}$ , $\text{m}^{-1}$
<i>Dark Production Rates Determined In Situ Using Hydrolysis Rates or Models</i>					
Ulshöfer et al. [1996] <sup>c</sup>	MED coastal	July 1993	$0.38 \pm 0.39$	24	$0.48 \pm 0.27$
Ulshöfer et al. [1996] <sup>c</sup>	MED open ocean	July 1993	$0.55 \pm 0.15$	23	$0.17 \pm 0.10$
Ulshöfer [1995] <sup>c</sup>	NEA temp, open ocean	March 1992	$0.09 \pm 0.03$	13	0.18
Ulshöfer [1995] <sup>c</sup>	NEA temp, open ocean	Jan. 1994	$0.03 \pm 0.01$	11	$0.09 \pm 0.03$
Ulshöfer [1995] <sup>c</sup>	NEA temp, open ocean	Sept. 1994	$0.11 \pm 0.03$	15	$0.15 \pm 0.02$
Ulshöfer [1995] <sup>c</sup>	NWA subtr, shelf	Aug. 1994	$0.62 \pm 0.14$	30	0.05
Ulshöfer [1995] <sup>c</sup>	NWA temp, shelf	March 1995	$0.06 \pm 0.02$	14	$0.15 \pm 0.04$
Ulshöfer [1995] <sup>c</sup>	NWA subtr, open ocean	March 1995	$0.09 \pm 0.03$	20	$0.09 \pm 0.02$
Von Hobe et al. [1999] <sup>c</sup>	NEA temp, open ocean	July 1997	0.14	20	$0.11 \pm 0.02$
Von Hobe et al. [1999] <sup>c</sup>	NEA subtr, open ocean	July 1997	0.15	21	$0.10 \pm 0.02$
Von Hobe et al. [1999] <sup>c</sup>	NEA subtr, upwelling	July 1997	0.32	18	$0.29 \pm 0.01$
This work <sup>c</sup>	NWA subtr, open ocean	Aug. 1999	0.26	27	0.03
This work <sup>d</sup>	NWA subtr, open ocean	Aug. 1999	0.20	27	0.03
<i>Dark Production Rates Determined by Incubation Experiments</i>					
Flöck and Andreae [1996] <sup>c</sup>	MED open ocean	July 1993	$0.42 \pm 0.26$	23	$0.17 \pm 0.10$
Flöck and Andreae [1996] <sup>c</sup>	NEA temp, open ocean	Jan. 1994	$0.08 \pm 0.11$	11	$0.09 \pm 0.03$
Flöck [1996] <sup>c</sup>	NS	April 1994	$0.65 \pm 0.40$	7	$2.4 \pm 3.1$
Flöck [1996] <sup>c</sup>	NEA temp, open ocean	Sept. 1994	$0.02 \pm 0.10$	15	$0.15 \pm 0.02$
Flöck [1996] <sup>c</sup>	NWA subtr, shelf	Aug. 1994	$0.90 \pm 0.20$	30	0.05
This work <sup>d</sup>	NWA subtr, open ocean	Aug. 1999	$0.42 \pm 0.13$	29	0.03

<sup>a</sup> Also shown are sea surface temperature (SST) and absorbance at 350 nm ( $a_{350}$ ).

<sup>b</sup> MED, Mediterranean; NEA, northeast Atlantic; temp., temperate region ( $35^{\circ}$ – $50^{\circ}$ ); NWA, northwest Atlantic; NS, North Sea; subtr, subtropical region ( $20^{\circ}$ – $35^{\circ}$ ).

<sup>c</sup> Hydrolysis rate according to Elliot [1989].

<sup>d</sup> Hydrolysis rate according to Radford-Knoery and Cutter [1994].

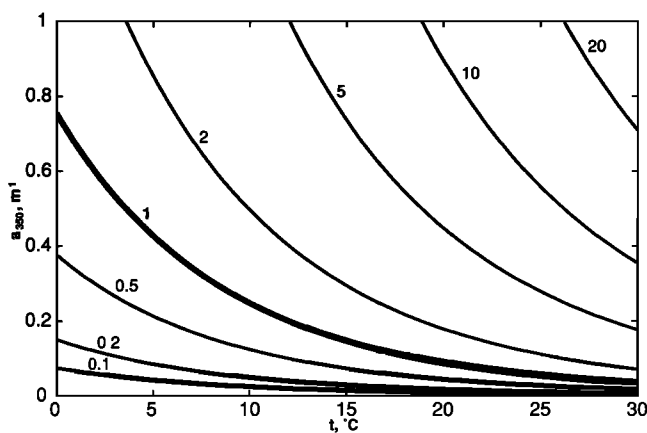


**Figure 5.** Contour plot of  $SR_{eq}$  as a function of temperature and  $a_{350}$ , with constant salinity = 36.0, pH = 8.1, and  $[COS]_{air} = 510$  ppt.

The equations suggest that COS dark production is first order with respect to  $a_{350}$ , a proxy for the concentration of CDOM, with a rate constant depending on temperature in Arrhenius fashion. However, as DOM concentration and biological activity in seawater show some covariance, this dependence does not yield conclusive evidence for either of the two proposed mechanisms.

#### 4. Global Implications of COS Dark Production

Our measurements in the Sargasso Sea show that the influence of dark production on marine COS concentrations is far from negligible. Under certain circumstances, depending on seawater temperature and CDOM content (or biological activity), dark production may, in fact, prevent the COS concentration from falling below values saturated with respect to the atmosphere even at times when there is no or very little photoproduction. For a given set of values for  $T$ ,  $S$ ,  $a_{350}$ , pH, and  $[COS]_{air}$  an equilibrium saturation ratio  $SR_{eq}$  can be defined that represents the COS saturation ratio that would exist if dark production and hydrolysis were balanced with no photoproduction:

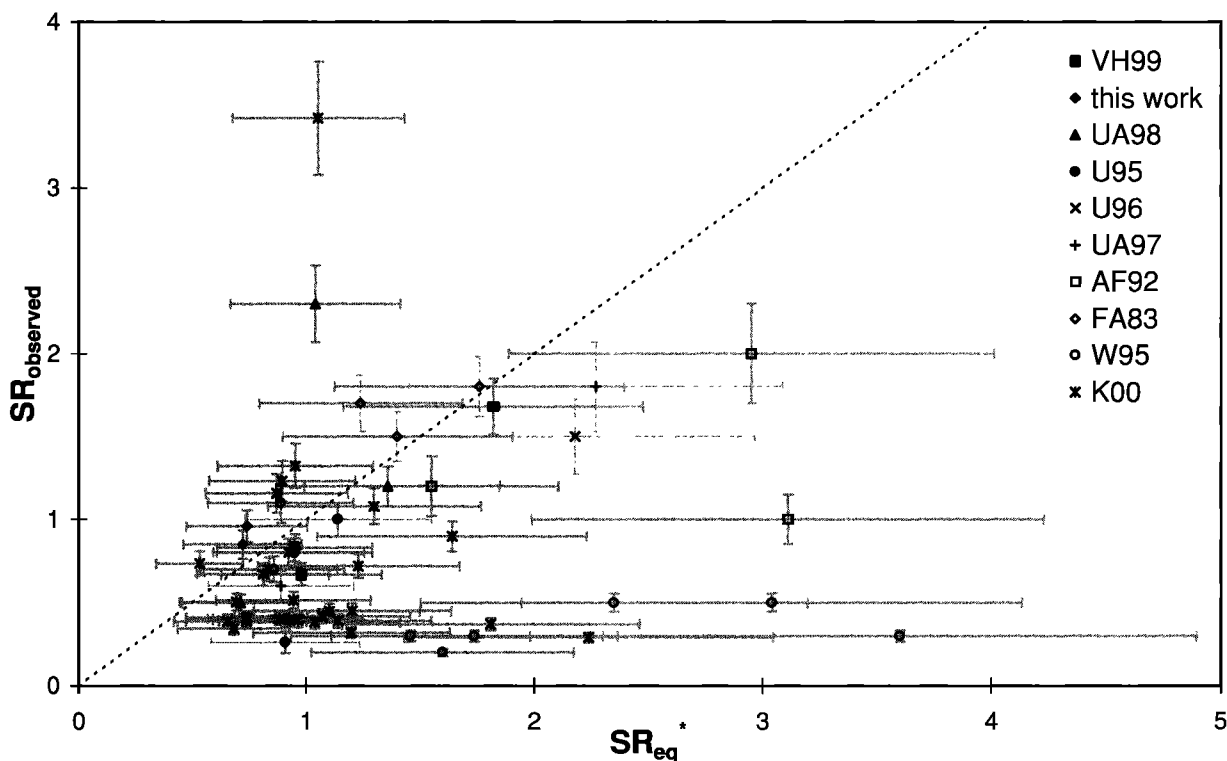
$$SR_{eq} = \frac{q(T, a_{350})/k_h(T, S, pH)}{[COS]_{air}/H(T, S)}, \quad (4)$$

Figure 4, a better fit with  $r^2 = 0.93$  is obtained, and the equation becomes

$$\ln(q/a_{350}) = 55.8 - 16200 T^{-1}, \quad (3)$$

with a standard error of the estimate for  $q$  of 36%.

where  $q$  is calculated according to (3),  $k_h$  is calculated according to Elliott et al. [1989], and  $H$  is calculated according to Ulshöfer et al. [1995]. A contour plot of  $SR_{eq}$  for different values of  $T$  and  $a_{350}$  is shown in Figure 5. The influence of  $S$  (set to 36.0 in Figure 5) is



**Figure 6.** Comparison of morning SR values observed during several cruises and  $SR_{eq}^*$  values calculated for the reported conditions. Horizontal error bars show the 36% error calculated for  $q$  (from (3)), which is much larger than the errors associated with  $k_h$ ,  $H$ , and  $k_w$ . Vertical error bars represent the precision of the COS measurements for the cited cruises.  $SR_{eq}^*$  is calculated using reported cruise averages or climatological averages (AF92, FA83, and W95) for  $T$ ,  $S$ , and  $a_{350}$ . References for the data sets are AF92, Andreae and Ferek [1992]; FA83, Ferek and Andreae [1983]; K00, Kettle et al. [2001]; U95, Ulshöfer et al. [1995]; U96, Ulshöfer et al. [1996]; UA98, Ulshöfer and Andreae [1998]; UA97, Uher and Andreae [1997]; VH99, Von Hobe et al. [1999]; W95, Weiss et al. [1995].



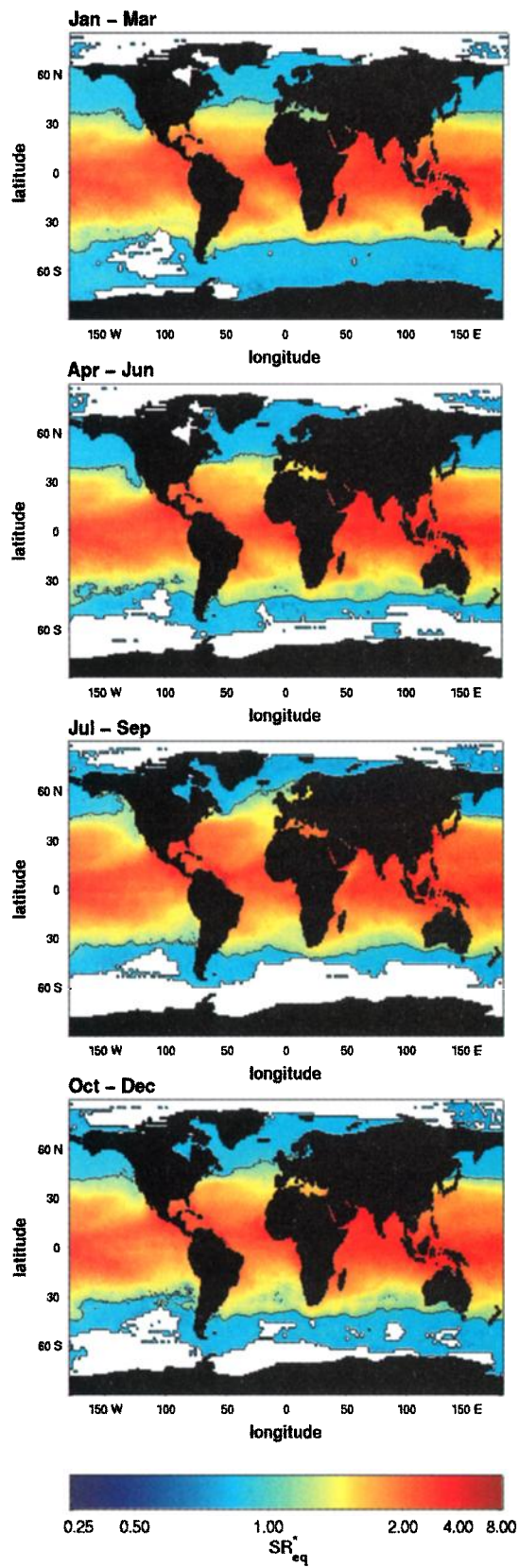


**Plate 1.** Global maps of  $SR_{eq}^*$  (seasonal averages). White indicates missing input variables. Black contour line shows  $SR_{eq}^* = 1$ , i.e., equilibrium with the atmosphere.

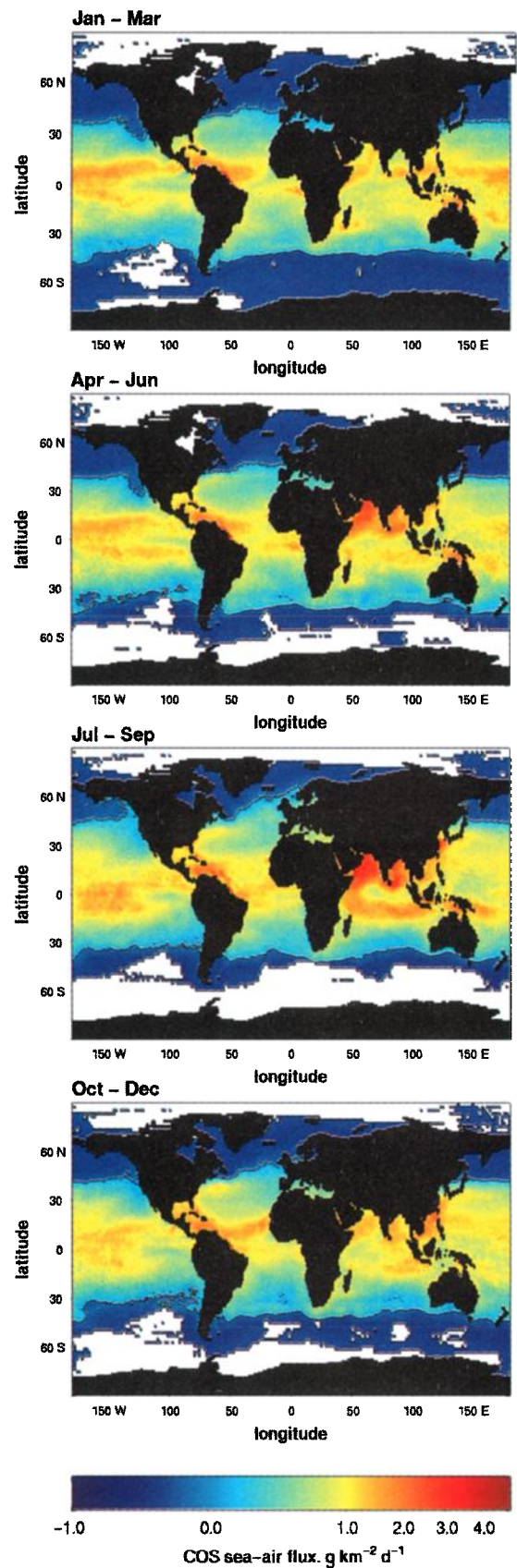


**Plate 2.** Global maps of  $F_d$  (seasonal averages). White indicates missing input variables. Black contour line denotes  $F_d = 0$ .

much less significant, and the variability of pH and  $[\text{COS}]_{\text{air}}$  under open ocean conditions is assumed to be small, and values were fixed at 8.1 and 510 ppt. The increase of  $\text{SR}_{\text{eq}}^*$  with  $a_{350}$  is easily rationalized by the linear relationship between  $q$  and  $a_{350}$  ((2) and (3)).  $\text{SR}_{\text{eq}}^*$  increases with  $T$  because the temperature dependence of  $q$  is steeper than that of  $k_h$  (i.e.,  $q$  has a higher activation energy) and because  $H$  also increases with  $T$ .

In cases where  $\text{SR}_{\text{eq}}^*$  is very different from 1 and wind speeds are moderately high, gas exchange with the atmosphere cannot be ignored, and (4) becomes

$$\text{SR}_{\text{eq}}^* = \frac{\frac{q(T, a_{350})}{[\text{COS}]_{\text{air}}/H(T, S)} + k_w/\Delta}{k_h(T, S, \text{pH}) + k_w/\Delta}, \quad (5)$$

where  $k_w$  is calculated as described in section 3.1 and  $\Delta$  is the thickness of the surface layer where the concentration is immediately influenced by gas exchange. Strictly, vertical mixing should also be taken into consideration, but as vertical gradients in  $[\text{COS}]_{\text{aq}}$  are usually low in the morning, it is ignored.

Values of  $\text{SR}_{\text{eq}}^*$  determined this way are compared to morning SR values measured in various ocean areas (Figure 6).  $\Delta$  is taken to be 3 m, approximately the value of the seawater inlet of most research ships. Most observations and theoretical values do agree within the range of the errors, with only a few larger deviations. It should be noted that the actual  $T$ ,  $S$ , and  $a_{350}$  during measurements may vary from the average values used to create Figure 6, which may be the cause of some of the deviations, especially where climatological data had to be used.

Global maps of surface  $\text{SR}_{\text{eq}}^*$  values for different seasons (Plate 1) can be generated by applying (5) to globally gridded climatological data sets of  $T$ ,  $S$ ,  $u$ , and  $a_{350}$  (keeping  $\text{pH} = 8.1$  and  $[\text{COS}]_{\text{air}} = 510$  ppt fixed and using  $\Delta = 1$  m). The  $1^\circ$  by  $1^\circ$  fields of  $T$  and  $S$  were obtained from *Levitus* [1982], and climatological wind fields for  $u$  were obtained from COADS1 (see Table 1). As no global data for CDOM absorbance were available, it was estimated from chlorophyll  $a$  concentrations (Sea-viewing Wide Field-of-view Sensor (SeaWiFS) remotely sensed data obtained from <http://daac.gsfc.nasa.gov>) using a formulation by *Kettle et al.* [2001]:

$$a_{300} = 0.429 + 0.079 \log_e[\text{CHL}_a], \quad (6)$$

where  $[\text{CHL}_a]$  is the chlorophyll  $a$  concentration in  $\text{mg m}^{-3}$ . *Kettle et al.* [2001] derived this formula from an extensive data set measured along an Atlantic meridional transect in 1997 with  $r^2 = 0.45$ . Although it agrees reasonably well with most other data sets, there remain large uncertainties, and for some regions and seasons, significant errors may be introduced by using (6) (see *Kettle et al.* [2001] for a more detailed description on the nature and magnitude of these uncertainties). To calculate  $a_{350}$  from  $a_{300}$ , a formulation by *Prieur and Sathyendranath* [1981], based on a spectral slope of 0.014, was used:

$$a_{\lambda_2} = a_{\lambda_1} e^{-0.014(\lambda_2 - \lambda_1)}, \quad (7)$$

The spectral slope is an average value but should give a good approximation for most of the world ocean except for some coastal regions.

Plate 1 shows that even with no photochemical COS production, most tropical and subtropical ocean areas are predicted to be oversaturated with COS, with  $\text{SR}_{\text{eq}}^*$  of up to  $\sim 8$ . Using the same parameterization as described in 3.1, COS fluxes can be calculated (Plate 2). Integrating over the entire ocean and a timescale of 1 year gives an annual flux of  $0.056 \text{ Tg COS yr}^{-1}$ .

The values plotted in the maps in Plates 1 and 2 and, subsequently, the global flux value should be treated with caution: neglecting vertical mixing, the choice of  $\Delta$  and, especially, the inexact values of  $a_{350}$  obtained from (6) and (7) introduce a large degree of uncertainty. Measurements [e.g., *Kettle et al.*, 2001;

*Weiss et al.*, 1995; this paper] suggest that particularly the values of  $\text{SR}_{\text{eq}}^*$  and COS flux predicted for some tropical areas are probably somewhat lower than predicted by (5), one possible reason being CDOM fading that is not accounted for by the approximation from chlorophyll. A better knowledge of global CDOM absorption fields would certainly help to improve the estimates. However, because taking into account photoproduction will definitely lead to higher SR values and fluxes, it is probably a reasonable assumption to take the estimated  $0.056 \text{ Tg COS yr}^{-1}$  as the lower limit for estimates of the global COS flux.

**Acknowledgments.** We thank O. Zafriou for the organization of the campaign and the crew of the R/V *Endeavor* for their support during the cruise and for providing the meteorological data and seawater parameters. Finally, we thank Carol Strametz and two anonymous reviewers for helpful comments on the manuscript. The R/V *Endeavor* cruise was funded under NSF grants OCE-9811208 to O. Zafriou and OCE-9815190 to G. Cutter. This work was supported by the Max Planck Society. It was part of the doctoral studies of M. Von Hobe at the University of East Anglia, Norwich, England.

## References

- Andreae, M. O., and P. J. Crutzen, Atmospheric aerosols: Biogeochemical sources and role in atmospheric chemistry, *Science*, 276, 1052–1058, 1997.
- Andreae, M. O., and R. J. Ferek, Photochemical production of carbonyl sulfide in seawater and its emission to the atmosphere, *Global Biogeochem. Cycles*, 6, 175–183, 1992.
- Bandy, A. R., D. C. Thornton, D. L. Scott, M. Lalevic, E. E. Lewin, and A. R. Driedger, III, A time series for carbonyl sulfide in the Northern Hemisphere, *J. Atmos. Chem.*, 14, 527–534, 1992.
- Broecker, W., and T. Peng, Gas exchange rates between air and sea, *Tellus*, 26, 21–35, 1974.
- Butler, J. H., J. W. Elkins, C. M. Brunson, K. B. Egan, T. M. Thompson, T. J. Conway, and B. D. Hall, Trace gases in and over the west Pacific and Indian Oceans during the El Niño Southern Oscillation event of 1987, Air Resour. Lab., Silver Spring, Md., 1988.
- Chin, M., and D. D. Davis, A reanalysis of carbonyl sulfide as a source of stratospheric background sulfur aerosol, *J. Geophys. Res.*, 100, 8993–9005, 1995.
- Clayton, T., and R. Byrne, Spectrophotometric seawater pH measurements: Total hydrogen ion concentration scale calibration of m-cresol purple and at sea results, *Deep Sea Res.*, 40, 2115–2129, 1993.
- Crutzen, P. J., The possible importance of CSO for the sulfate layer of the stratosphere, *Geophys. Res. Lett.*, 3, 73–76, 1976.
- Elliott, S., E. Liu, and F. S. Rowland, Rates and mechanisms for the hydrolysis of carbonyl sulfide in natural waters, *Environ. Sci. Technol.*, 23, 458–461, 1989.
- Erickson, D. J., A stability dependent theory for air-sea gas exchange, *J. Geophys. Res.*, 98, 8471–8488, 1993.
- Ferek, R. J., and M. O. Andreae, The supersaturation of carbonyl sulfide in surface waters of the Pacific Ocean off Peru, *Geophys. Res. Lett.*, 10, 393–396, 1983.
- Ferek, R. J., and M. O. Andreae, Photochemical production of carbonyl sulfide in marine surface waters, *Nature*, 307, 148–150, 1984.
- Flöck, O., Entstehung, Abbau und vertikale Verteilung von Carbonylsulfid und Methylmercaptan im Wasser der Ozeane, Ph.D. thesis, Johannes-Gutenberg-Universität, Mainz, Germany, 1996.
- Flöck, O., and M. O. Andreae, Photochemical and non-photochemical formation and destruction of carbonyl sulfide and methyl mercaptan in ocean waters, *Mar. Chem.*, 54, 11–26, 1996.
- Flöck, O. R., M. O. Andreae, and M. Dräger, Environmentally relevant precursors of carbonyl sulfide in aquatic systems, *Mar. Chem.*, 59, 71–85, 1997.
- Kettle, A., T. Rhee, M. Von Hobe, A. Poulton, J. Aiken, and M. Andreae, Rethinking the flux of volatile sulfur gases to the atmosphere, *J. Geophys. Res.*, 106, 12, 193–12, 209, 2001.
- Leung, P., and M. Hoffmann, Kinetics and mechanism of autooxidation of 2-mercaptoethanol catalysed by cobalt(II)-4,4',4'',4-tetrasulfophthalocyanine in aqueous solution., *Environ. Sci. Technol.*, 22, 275–282, 1988.
- Levitus, S., *Climatological Atlas of the World Ocean*, Natl. Oceanic and Atmos. Admin., Silver Spring, Md., 1982.
- Liss, P. S., and L. Merlivat, Air-sea gas exchange rates: Introduction and synthesis, in *The Role of Air-Sea Exchange in Geochemical Cycling*,

- edited by P. Buat-Ménard, pp. 113–127, D. Reidel, Norwell, Mass., 1986.
- Liss, P. S., and P. G. Slater, Flux of gases across the air-sea interface, *Nature*, **247**, 181–184, 1974.
- Millero, F., Thermodynamics of the carbon dioxide system in the oceans, *Geochim. Cosmochim. Acta*, **59**, 661–677, 1995.
- Najjar, R. G., D. J. Erickson, III, and S. Madronich, Modeling the air-sea fluxes of gases formed from the decomposition of dissolved organic matter: Carbonyl sulfide and carbon monoxide, in *The Role of Nonliving Organic Matter in the Earth's Carbon Cycle*, edited by R. G. Zepp and C. Sonntag, pp. 107–132, John Wiley, New York, 1995.
- Nightingale, P., G. Malin, C. Law, A. Watson, P. Liss, M. Liddicoat, J. Boutin, and R. Upstill-Goddard, In situ evaluation of air-sea gas exchange parameterizations using novel conservative and volatile tracers, *Global Biogeochem. Cycles*, **14**, 373–388, 2000.
- Ohno, A., Thiols, in *Organic Chemistry of Sulfur*, edited by S. Oae, Plenum, New York, 1977.
- Pos, W. H., D. D. Riemer, and R. G. Zika, Carbonyl sulfide (OCS) and carbon monoxide (CO) in natural waters: Evidence of a coupled photo-production pathway, *Mar. Chem.*, **62**, 89–101, 1998.
- Prieur, L., and S. Sathyendranath, An optical classification of coastal and oceanic waters based on the specific spectral absorption curves of phytoplankton pigments, dissolved organic matter, and other particulate materials., *Limnol. Oceanogr.*, **26**, 671–689, 1981.
- Radford-Knoery, J., and G. A. Cutter, Determination of carbonyl sulfide and hydrogen sulfide species in natural waters using specialized collection procedures and gas chromatography with flame photometric detection, *Anal. Chem.*, **65**, 976–982, 1993.
- Radford-Knoery, J., and G. A. Cutter, Biogeochemistry of dissolved hydrogen sulfide species and carbonyl sulfide in the western North Atlantic Ocean, *Geochim. Cosmochim. Acta*, **58**, 5421–5431, 1994.
- Solomon, S., R. W. Sanders, R. R. Garcia, and J. G. Keys, Increased chlorine dioxide over Antarctica caused by volcanic aerosols from Mount Pinatubo, *Nature*, **363**, 245–248, 1993.
- Turco, R. P., R. C. Whitten, O. B. Toon, J. B. Pollack, and P. Hamill, OCS, stratospheric aerosols and climate, *Nature*, **283**, 283–286, 1980.
- Uher, G., and M. O. Andreae, The diel cycle of carbonyl sulfide in marine surface waters: Field study results and a simple model, *Aquat. Geochem.*, **2**, 313–344, 1997.
- Ulshöfer, V. S., Photochemische Produktion von Carbonylsulfid im Oberflächenwasser der Ozeane und Gasaustausch mit der Atmosphäre, Ph.D. thesis, Ruprecht-Karls-Univ., Heidelberg, Germany, 1995.
- Ulshöfer, V. S., and M. O. Andreae, Carbonyl sulfide (COS) in the surface ocean and the atmospheric COS budget, *Aquat. Geochem.*, **3**, 283–303, 1998.
- Ulshöfer, V. S., O. R. Flöck, G. Uher, and M. O. Andreae, Photochemical production and air-sea exchange of carbonyl sulfide in the eastern Mediterranean Sea, *Mar. Chem.*, **53**, 25–39, 1996.
- Ulshöfer, V. S., G. Uher, and M. O. Andreae, Evidence for a winter sink of atmospheric carbonyl sulfide in the northeast Atlantic Ocean, *Geophys. Res. Lett.*, **22**, 2601–2604, 1995.
- Von Hobe, M., A. J. Kettle, and M. O. Andreae, Carbonyl sulphide in and over seawater: Summer data from the northeast Atlantic Ocean, *Atmos. Environ.*, **33**, 3503–3514, 1999.
- Von Hobe, M., T. Kenntner, F. Helleis, L. Sandoval-Soto, and M. Andreae, Cryogenic trapping of carbonyl sulphide without using expendable cryogenes, *Anal. Chem.*, **72**, 5513–5515, 2000.
- Wanninkhof, R., Relationship between wind speed and gas exchange over the ocean, *J. Geophys. Res.*, **97**, 7373–7382, 1992.
- Watts, S., The mass budgets of carbonyl sulfide, dimethyl sulfide, carbon disulfide and hydrogen sulfide, *Atmos. Environ.*, **34**, 761–779, 2000.
- Weiss, P. S., J. E. Johnson, R. H. Gammon, and T. S. Bates, Reevaluation of the open ocean source of carbonyl sulfide to the atmosphere, *J. Geophys. Res.*, **100**, 20,092–23,083, 1995.
- Weiss, R. F., F. A. Van Woy, and P. K. Salameh, Surface water and atmospheric carbon dioxide and nitrous oxide observations by shipboard automated gas chromatography: Results from expeditions between 1977 and 1990, Carbon Dioxide Inf. Anal. Cent., Oak Ridge Natl. Lab., Oak Ridge, Tenn., 1992.
- Zhang, L., R. S. Walsh, and G. A. Cutter, Estuarine cycling of carbonyl sulfide: Production and sea-air flux, *Mar. Chem.*, **61**, 127–142, 1998.

M. O. Andreae and A. J. Kettle, Biogeochemistry Department, Max Planck Institute for Chemistry, PO Box 3060, D-55020 Mainz, Germany.

G. A. Cutter, Department of Ocean, Earth, and Atmospheric Sciences, Old Dominion University, 4600 Elkhorn Avenue, Norfolk, VA 23529-0276, USA.

M. Von Hobe, Forschungszentrum Jülich, ICG-I, D-52425 Jülich, Germany. (m.von.hobe@fz-juelich.de)

(Received July 25, 2000; revised August 22, 2001; accepted August 27, 2001.)